UNIVERSITY OF BUCHAREST
FACULTY OF CHEMISTRY
DOCTORAL SCHOOL IN CHEMISTRY

DOCTORAL THESIS

THE DESIGN OF NOVEL NITRONYL NITROXIDE LIGANDS FOR THE SYNTHESIS OF HETEROSPIN COMPLEXES

ABSTRACT

PhD Student:

Mihai Florin RĂDUCĂ

Supervisor:

Acad. Marius ANDRUH

2025

The present thesis, entitled “The Design of Novel Nitronyl Nitroxide Ligands for the Synthesis of Heterospin Complexes”, aims to present original contributions to the development of new nitronyl nitroxide ligands and their corresponding complexes.

The synthesis of paramagnetic organic molecules represents an intriguing and developing subject of the current research in chemistry. Among the organic radicals employed as ligands in coordination chemistry, nitronyl nitroxides have attracted considerable attention, mainly due of their significant role in the field of molecular magnetism and due to their versatility as ligands. First synthesized by Ullman in the late 1960s, nitronyl nitroxide (NN) molecules have since been widely employed in the preparation of complexes that have been investigated for their magnetic properties.

The distinctive paramagnetic nature of NN ligands enables the formation of heterospin complexes with 2p–3d, 2p–4f, and even 2p–3d–4f spin configurations, as well as other possible combinations, leading to a wide variety of molecular topologies. Furthermore, symmetric molecules can be dissymmetrized by converting one of two formyl groups into a nitronyl nitroxide moiety. New ligands may also be obtained through Schiff base reactions between diamagnetic amine molecules and paramagnetic nitronyl nitroxide species. In addition, nitronyl nitroxide molecules bearing a CH_2–Cl pendant arm can be grafted onto various substrates *via* N-, O-, or C-alkylation. Consequently, two main strategies for designing paramagnetic ligands have been developed: (i) the synthesis of molecules containing coordinating functionalities and an aldehyde group, followed by conversion of the aldehyde into a nitronyl nitroxide moiety; and (ii) the grafting of a preformed nitronyl nitroxide unit onto a substrate through alkylation reactions.

The thesis is organized into two main parts: the first focuses on the theoretical concepts addressed in this work, together with an overview of the current state of the radical chemistry focused on coordination complexes; the second presents the original experimental results, with each part being divided into several chapters. The principal research directions are illustrated in brief in Scheme 1.

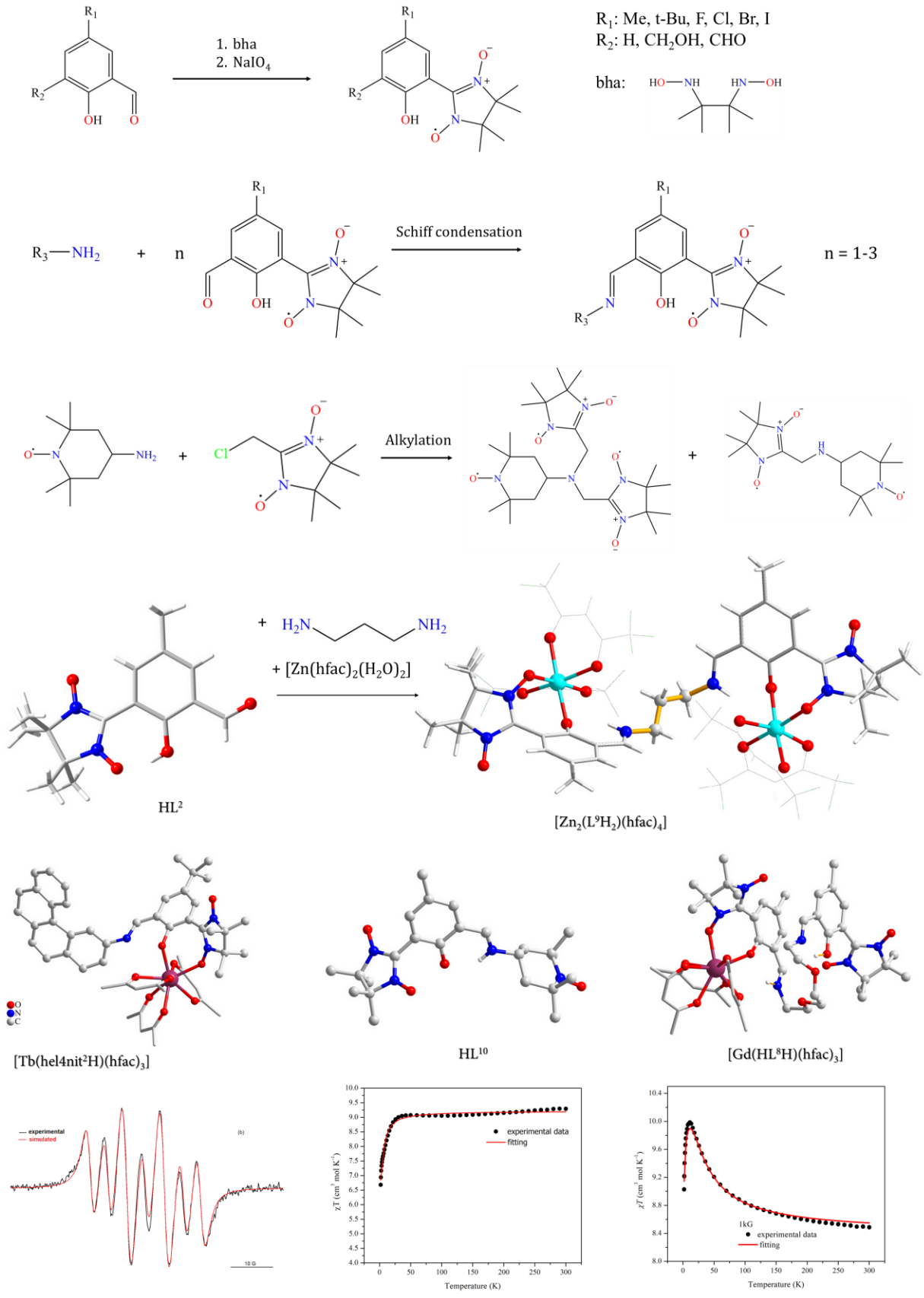

Scheme 1. Graphical abstract of the main topics of the thesis.

The theoretical part is divided into two chapters. Chapter 1 concerns paramagnetic organic molecules with emphasis to nitronyl nitroxide radicals and their ability to form coordination compounds with diverse nuclearity and spin topology.

Most organic molecules are diamagnetic due to paired electrons, but the discovery of the first stable organic radical in 1900 generated the study of open-shell organic systems with unpaired electrons. These organic radicals have enabled important applications in polymer science, surface chemistry, and particularly magnetochemistry. In organic magnetic materials, isotropic exchange interactions primarily govern magnetic behavior, which can be described using an effective spin Hamiltonian. Magnetic interactions may be ferromagnetic or antiferromagnetic depending on the overlap of singly occupied molecular orbitals. The design of organic magnetic materials depends on the stability of radical units, the mechanisms of magnetic coupling, and the transmission of interactions through the material. Both intra- and intermolecular interactions contribute to magnetic behavior, with supramolecular forces such as hydrogen bonding, π–π stacking, and halogen bonding playing a key role in assembling magnetic structures.

The nitronyl nitroxide (NN) radical contains two equivalent NO groups, enabling it to function as a versatile paramagnetic ligand that can act as a terminal ligand or bridge metal ions to form one-dimensional chain structures. The unpaired electron localized on the NO units promotes magnetic exchange interactions with coordinated paramagnetic metal ions. Since the 1980s, NN-bridged 3d and 4f metal chain compounds have been extensively studied, with some exhibiting three-dimensional magnetic ordering. Depending on the substituent (R), NN can also coordinate as a monodentate ligand, and these stable radicals are characterized by a distinctive dark-violet color arising from n–π* electronic transitions. The imino nitroxide (IN) radical is structurally related to NN exhibiting only one NO group (Scheme 2).

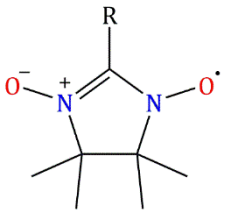

NN

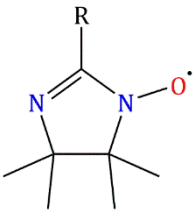

IN

Scheme 2. Structures of nitronyl nitroxide (NN) and imino nitroxide (IN) radicals.

The coordination chemistry of nitronyl nitroxides continues to yield a wide variety of unique bistable magnetic systems. The possible coordination modes involving the two

oxygen atoms of the radical were first described by Paul Ray in 1989, and numerous compounds have since been reported featuring monodentate, bridging (exobidentate), and mixed coordination modes connecting multiple metal ions (Scheme 3).

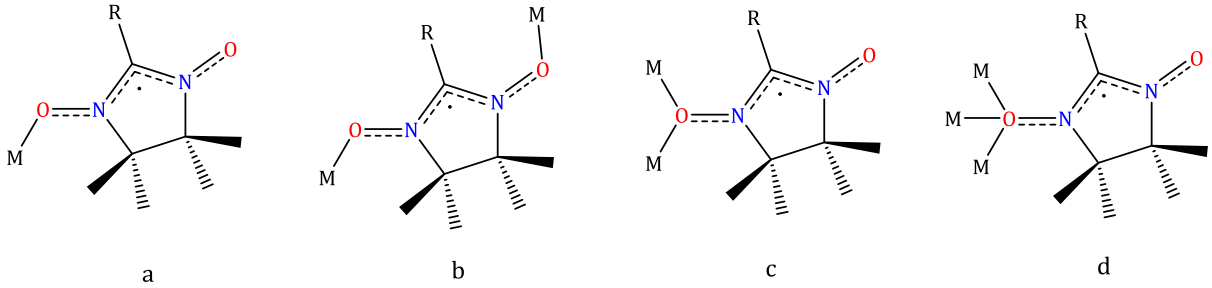

Scheme 3. Scheme of the binding modes of the N-O unit of nitronyl nitroxide radicals: (a) monodentate, (b) exobidentate bridge, (c) μ_2-O bridge, (d) μ_3-O bridge.

The following chapter gives several examples from the literature of heterospin complexes bearing 3d, 4f and 3d-4f metal ions along with a short discussion of the structural features and magnetic properties. The chapter concludes that paramagnetic NN ligands are valuable ligands because of their ability to form complexes with a wide range of metal ions. Their structures can be modified with different coordinating groups, enabling multiple coordination modes and making them ideal for constructing complexes with varied topologies, nuclearities and dimensionalities.

***

The section detailing original contributions consists of four chapters.

Chapter 1 details the design and structural characteristics of the ligands utilized throughout this research. Additionally, it discusses specific organic molecules synthesized as a proof of concept.

The precursor 2,6-bis(hydroxymethyl)-p-cresol **(HL^{a})** is a versatile starting material that can be selectively oxidized into either a monoaldehyde (**HL^{b}**) or a dialdehyde (**HL^{c}**). These aldehydes serve two key synthetic purposes: they can react with primary amines to form compartmental Schiff ligands, or they can be converted into nitronyl nitroxide radicals through a two-step sequence known as Ullman's protocol. In this sequence, the aldehyde is first condensed with 2,3-bis(hydroxylamino)-2,3-dimethylbutane (**bha**) to create an imidazolidine-1,3-diol intermediate (**HΨ^{1}**). This intermediate is then oxidized with $NaIO_4$ to produce the target nitronyl nitroxide radical (**HL^{1}**), which is typically accompanied by an imino nitroxide equivalent (**HΛ^{1}**), and purified *via* column chromatography. Likewise in the case of transforming the dialdehyde (**HL^{c}**) into the corresponding radical **HL^{2}**. Single crystals of **HL^{2}** suitable for X-ray diffraction were obtained by evaporating diethyl ether under

reduced pressure using a rotary evaporator. **HL²** crystallizes in the monoclinic crystal system, I2/α space group (Figure 1). The presence of a formyl functional group in **HL²** enables further ligand derivatization through a straightforward Schiff base condensation, thereby introducing an additional coordination site.

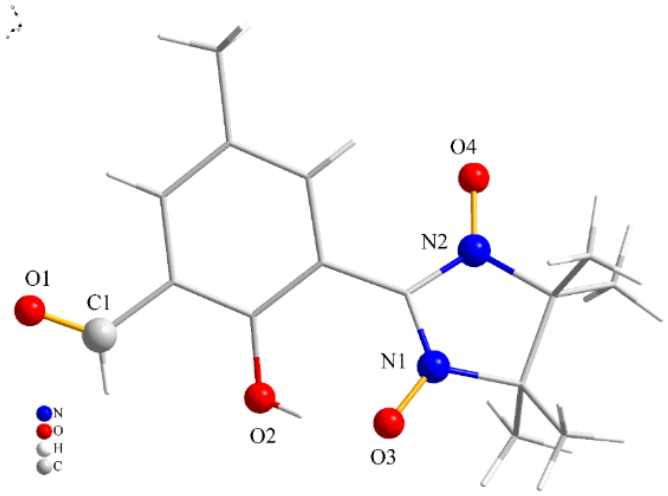

Figure 1. View of the molecular structure of **HL²** determined by X-ray diffraction.

By using a facile and quasi-quantitative Schiff base condensation, starting from **HL²** two NN moieties were linked through various diamine spacers (*e.g.* 2,2′-(ethylenedioxy)bis(ethylamine) and 1,3-diaminopropane) to afford the diradical ligands **H₂L⁸** and **H₂L⁹**, respectively (Scheme 4).

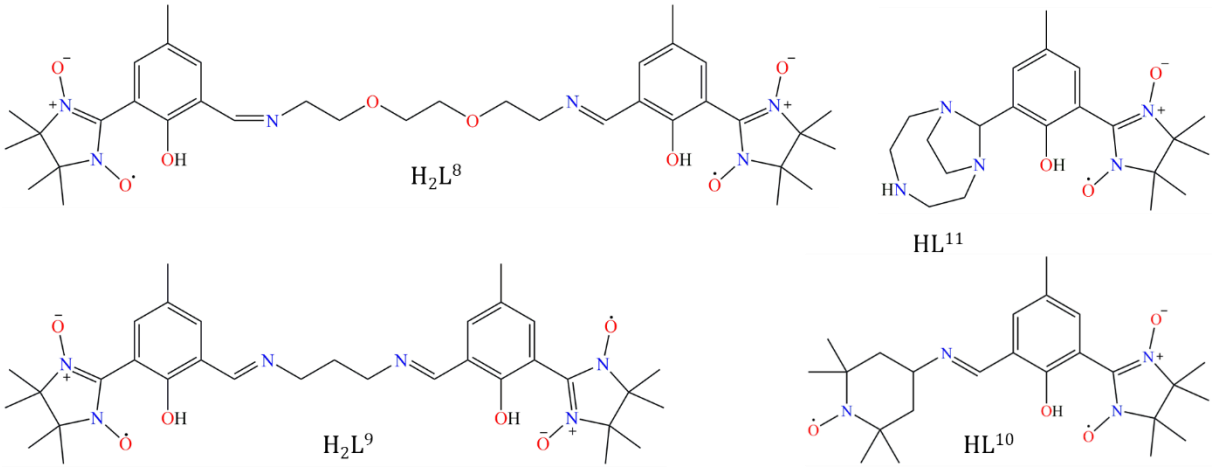

Scheme 4. The structures of mono and diradicals obtained *via* Schiff reactions.

The nature, length, and rigidity or flexibility of the spacer play a crucial role in the formation of complexes with different metal ions by modulating the available coordination sites, as well as in the design of molecular materials with potential applications as quantum gates. Moreover, a hetero-di-radical ligand, **HL¹⁰**, was synthesized using amino-TEMPO. *To the best of my knowledge, this represents the first molecular system combining TEMPO and*

NN radical moieties into the same molecule. The temperature dependence of the magnetic properties is presented in the form $\chi_M T$ vs. T for the diradical ligands **H_2L^8** and **HL^{10}** (Figure 2). In the case of the hetero-di-radical **HL^{10}** an antiferromagnetic behavior is observed. At 300 K, the $\chi_M T$ value is 0.749 $cm^3\ mol^{-1}\ K$, which is in excellent agreement with the theoretical value of 0.75 $cm^3\ mol^{-1}\ K$ expected for two non-interacting S = 1/2 radical centers. Upon cooling, the $\chi_M T$ product remains nearly constant down to 40 K, below which it decreases sharply, reaching 0.488 $cm^3\ mol^{-1}\ K$ at 1.8 K

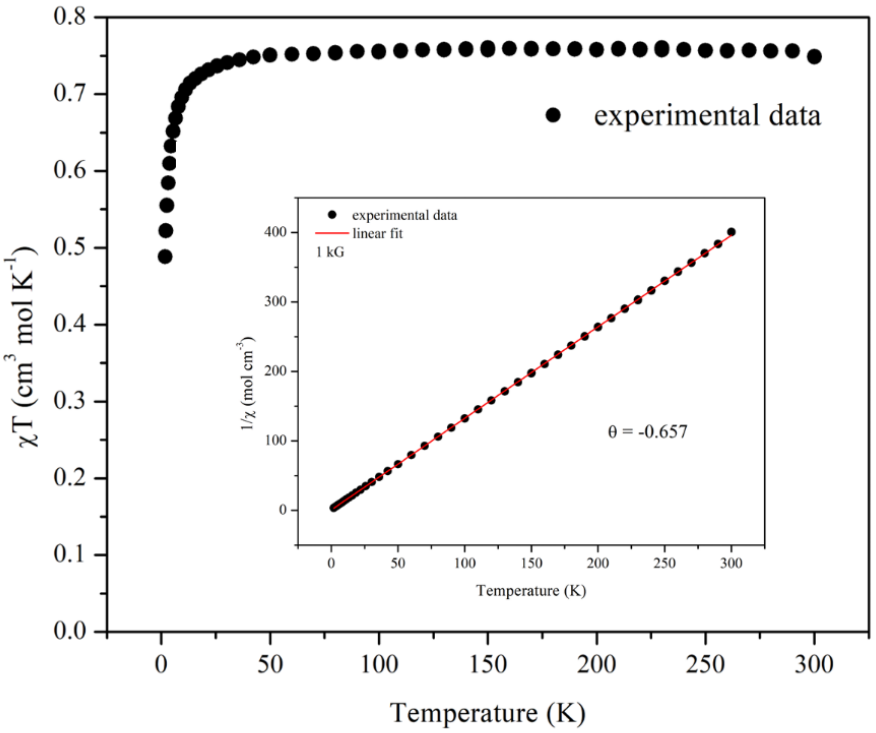

Figure 2. Temperature dependence the $\chi_M T$ product for the ligand **HL^{10}**. Insert $(\chi_M)^{-1}$ vs T plot.

Chapter 2 describes three families of dinuclear complexes with 4f metal ions, providing a comparative analysis of their structural similarities and differences. The magnetic properties of one specific series are evaluated. The byproducts identified during synthesis are discussed with a comprehensive analysis across four detailed subchapters.

The first family of compounds, $[Ln_2(L^1)_2(hfac)_4]$ where Ln = Y, Gd, Tb, Dy, has been extensively studied along with the products obtained during the optimization on the syntheses. Compounds $[Ln_2(L^1)_2(hfac)_4]$ are isostructural and consist of centrosymmetric dinuclear units, the lanthanide ions being bridged by the phenoxido groups arising from two single deprotonated radicals, $(\mathbf{L^1})^-$. Each lanthanide ion shows a coordination number of 8, with a square antiprism stereochemistry (Figure 3).

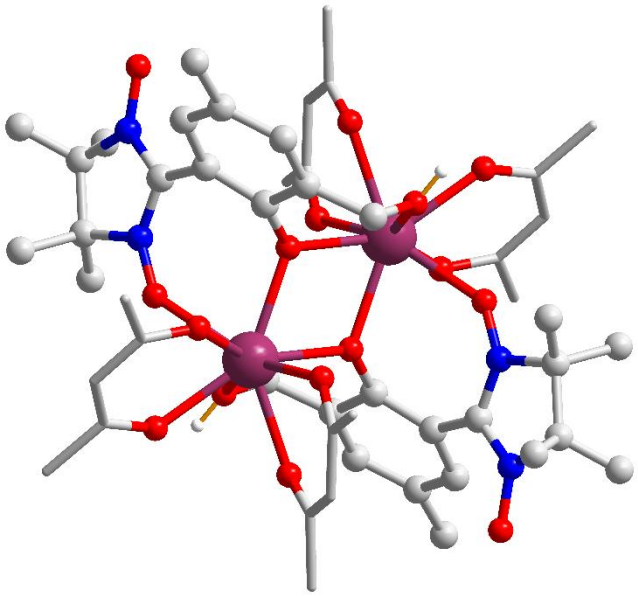

Figure 3. View of the molecular structures of $[Ln_2(L^1)_2(hfac)_4]$. A part of the hydrogen atoms and all fluorine atoms were removed for clarity.

The $\chi_M T$ vs T and M vs H behaviors for compounds $[Ln_2(L^1)_2(hfac)_4]$, where Ln = Gd (**2**), Tb (**3**), Dy (**4**), have been recorded. The $\chi_M T$ value at 300 K is 16.8 $cm^3mol^{-1}K$ for **2**, 24.1 $cm^3mol^{-1}K$ for **3**, and 28.9 $cm^3mol^{-1}K$ for **4**, in good agreement with those expected for the paramagnetic contributions of the metal ions (Gd(III), S = 7/2; Tb(III), J = 6, g_J = 3/2; Dy(III), J = 15/2, g_J = 4/3) and two S = ½ radicals in the absence of exchange interactions (*i.e.* **2**: 16.51; **3**: 24.39; **4**: 29.09 $cm^3mol^{-1}K$). For **2**, $\chi_M T$ remains constant between 300 and 80 K, when it starts to decrease reaching 10.5 $cm^3mol^{-1}K$ at 2 K. This behavior can be ascribed to overall antiferromagnetic interactions arising from the interplay of two exchange pathways, namely the Gd(III)-Gd(III) exchange interaction mediated by the two phenoxido bridges, and the Gd(III)-Rad interactions. The first one was found to be weak and antiferromagnetic in numerous compounds. On the other hand, the Gd(III)-NN exchange interactions were found both ferro- and antiferromagnetic, and are strongly influenced by the Gd-O-N and Gd-O-N-C angles, as well as the Gd–O distance. Exceptionally, *for the gadolinium dinuclear complex, **2**, the pulse EPR measurements revealed that phase memory times, T_m, about 1000 ns at 6 K* regardless of the magnetic field position. In contrast, the spin-lattice relaxation time, T_1, is considerably longer (ca. 3.7 ms) at the radical (observer position OP2) compared to the isolated Gd(III) ion (19.3 µs at OP1; 20.77 µs at OP3) (Figure 4).

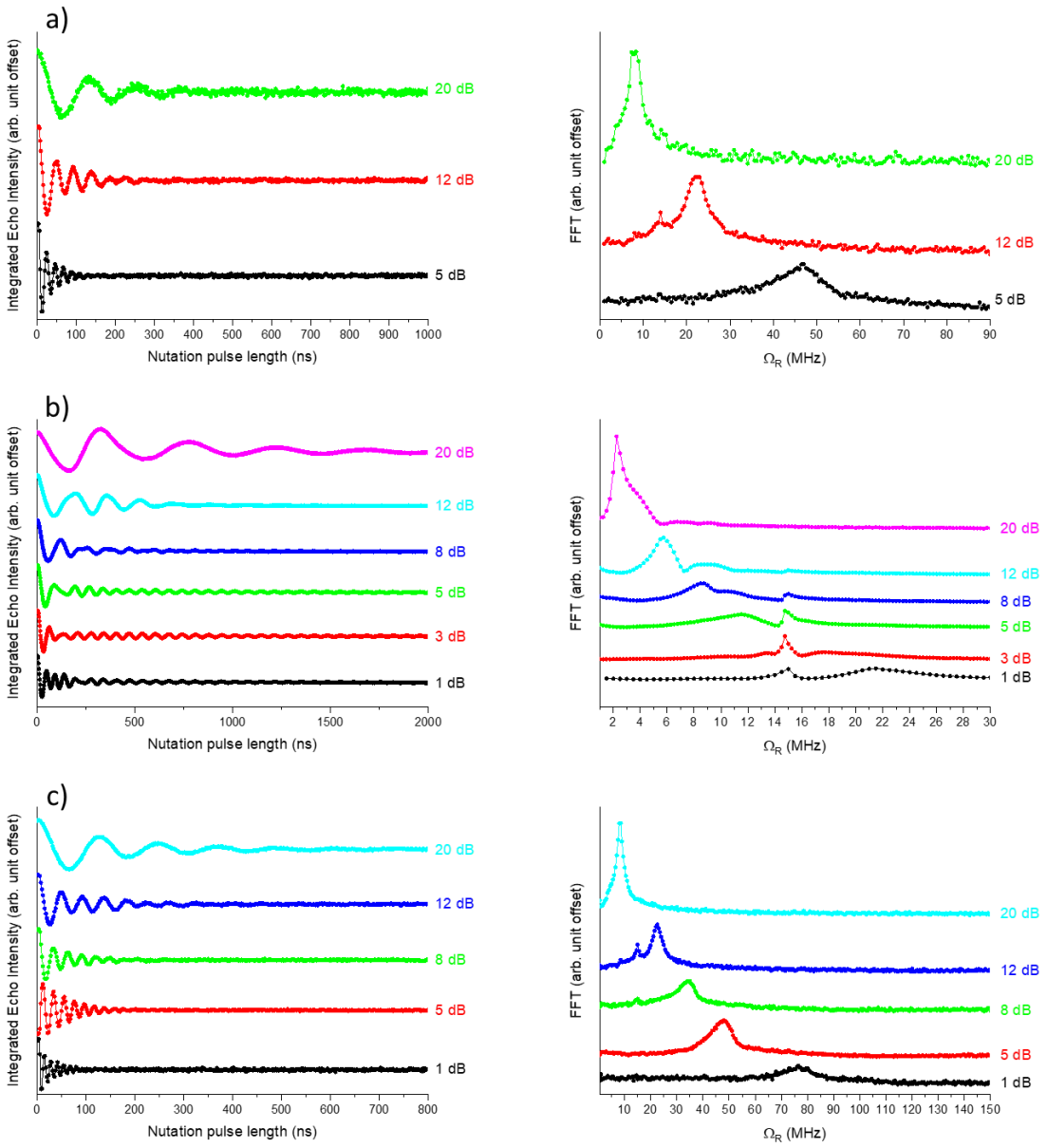

Figure 4. Rabi oscillations acquired with different microwave attenuations (left) and corresponding Fourier transforms (right) for a 1.2 mM methanol / toluene 9:1 (v/v) solution of **2** at 6 K (a) 3280G (OP1), (b) 3504 G (OP2) and (c) 3570 G (OP3). Solid lines are guide to the eye. The peak at around 15 MHz corresponds to the Larmor frequency of ^{1}H nucleus.

Chapter 3 presents a comparative analysis of two families of dinuclear complexes featuring transition metal ions. This evaluation includes also the investigation of several byproducts formed during their synthesis.

The two monoradicals, one decorated with a hydroxymethyl group (**HL^1**) and the other one with a formyl group (**HL^2**), have been used as ligands against Ni(II) and Zn(II) ions, resulting in binuclear complexes: $[Ni_2(L^1)_2(hfac)_2]$ **34**, $[Zn_2(L^1)_2(hfac)_2]$ **35**, $[Ni_2(L^2)_2(hfac)_2]$ **38-39**, $[Zn_2(L^2)_2(hfac)_2]$ **41**. In the case of compounds **34** and **41** two

crystalline phases were obtained: trigonal τγ- and triclinic τ-. The crystal structures of τγ-**34** and τ-**34**, consist of centrosymmetric binuclear units (Figure 5), the nickel ions being bridged by the phenoxido groups arising from two deprotonated radicals, $(\mathbf{L^1})^-$. Compound τγ-**34** crystalizes in trigonal crystal system, *R*-3 space group, and compound τ-**34** crystalizes in triclinic crystal system, *P*-1 space group. Short contacts are established between the radicalic oxygen from one binuclear unit with the same atom from the neighboring unit with in the case of τ-**34** (see Figure 5).

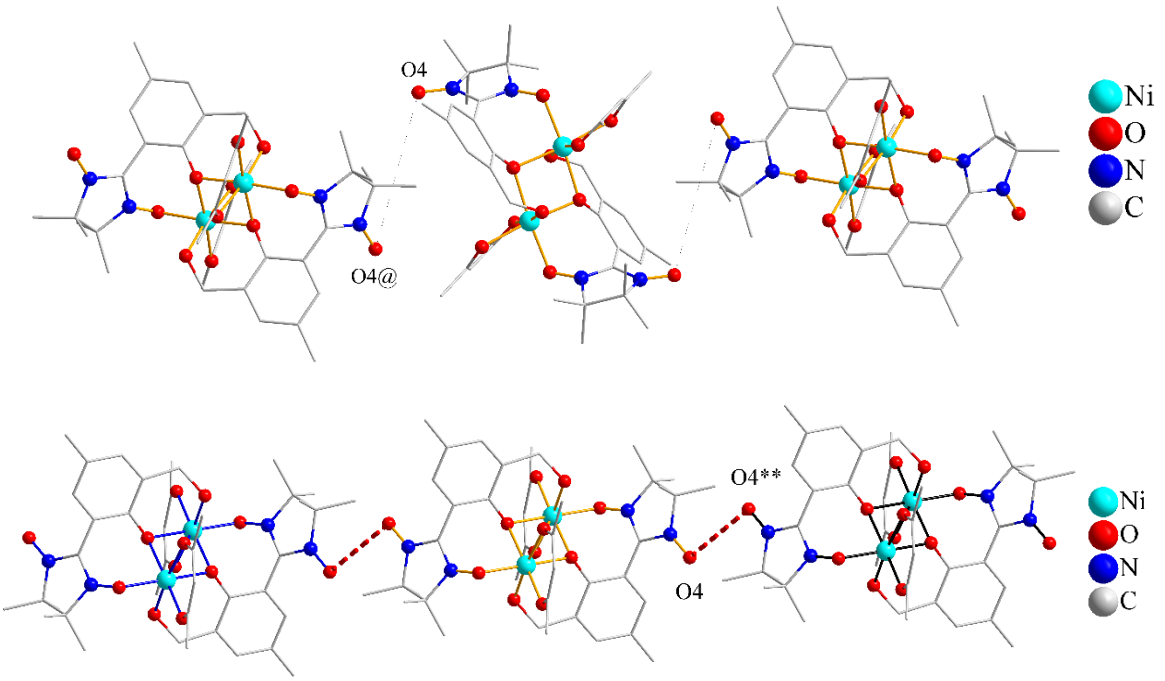

Figure 5. View of close contacts between the NN moieties of τγ-**34** (top) and τ-**34** (bottom). Hydrogen and fluorine atoms have been removed for clarity. Symmetry operations: @ = *y, 1-x+y, 1-z*; ** = *-x, -y, 1-z*. Distances are O4···O4@ = 5.94 Å and O4···O4** = 3.96 Å. In the case of compound **35** the distance O4···O4** is 4.14 Å.

The magnetic properties of compounds τγ-**34**, **35**, **38** and τγ-**41** have been investigated. At room temperature $\chi_M T$ values of 1.45 cm^3 K mol^{-1} for τγ-**34** and 1.96 cm^3 K mol^{-1} for **38** are obtained, which are significantly lower than the expected value of 2.75 cm^3 K mol^{-1} for two Ni(II) with $S_1 = S_2 = 1$ and two radicals with $S_3 = S_4 = {}^1/_2$. This value supports a strong antiferromagnetic interaction between the Ni(II) and Ni(II) ions mediated by the phenoxido groups. With lowering the temperature, a decrease of the $\chi_M T$ product can be observed, reaching a minimum at 110 K with values of 1.16 cm^3 K mol^{-1} and 1.30 cm^3 K mol^{-1} for τγ-**34** and **38**, respectively. Further cooling leads to an increase again and values of 1.35 cm^3 K mol^{-1} and 1.45 cm^3 K mol^{-1} at 2 K were observed. This behavior indicates competing exchange interaction within the complexes, which is further supported by the magnetization

measurements. At 2 K and 7 T saturation values of 2.41 $N\mu_B$ and 2.46 $N\mu_B$ are observed, significantly lower than the expected value of 6 $N\mu_B$ for uncoupled spin centers. No satisfactory simulation of the magnetic data could be achieved if only the interaction between the radical and the neighboring Ni(II) *via* the aminoxyl and between the Ni(II) ions *via* the phenoxido bridges was considered. Therefore, a third interaction was included in the model that involves the radical also interacting with the second Ni(II) ion. Good simulation of the data is obtained with J_1 = -47 cm^{-1}, J_2 = -117 cm^{-1} and J_3 = -106 cm^{-1} for τγ-**34** and J_1 = -25.5(2) cm^{-1}, J_2 = -71(2) cm^{-1} and J_3 = -71(2) cm^{-1} for **38.** This indicates that the radical is mainly located on the μ_2-phenoxido bridge than at the NN group. The $\chi_M T$ *vs* T plots for τγ-**34** and **38** are presented in Figure 6.

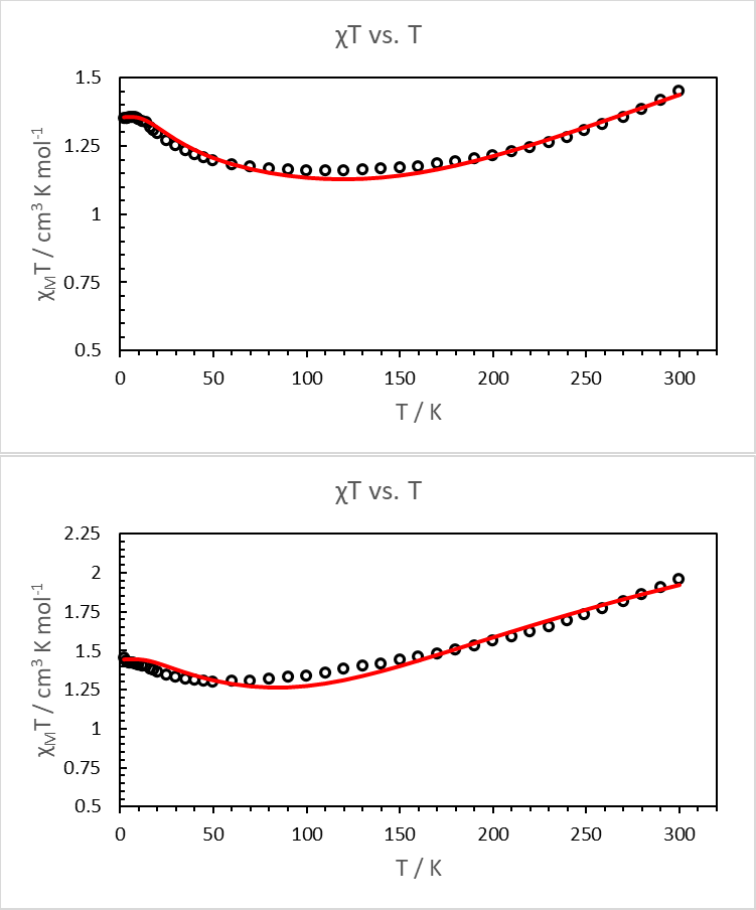

Figure 6. Magnetic behavior for τγ-**34** (up) and **38** (down).

Chapter 4 explores the diverse chemistry of 3d and 4f metal ions when coordinated with homo- and hetero-di-radicals synthesized *via* Schiff reactions.

The two homo-di-radicals $\mathbf{H_2L^8}$ cand $\mathbf{H_2L^9}$ and the hetero-di-radical $\mathbf{HL^{10}}$ were obtained by generating Schiff bases between $\mathbf{HL^2}$ and 2,2′-(ethylenedioxy)bis(ethylamine), 1,3-diaminopropane and 4-amino-TEMPO, respectively.

Dinuclear complexes, $[M_2(L^9H_2)(hfac)_4]$, were formed using transitional metal ions, M = Mn (**54**), Co (**55**), Ni (**56**), Zn (**57**). Compounds **55-57** are isostructural whereas the manganese derivative (**54**) crystalize with a solvent molecule and presents a different conformation of the ligand. Compound **[**$Mn_2(L^9H_2)(hfac)_4]\cdot CH_2Cl_2$ (**54**) crystalizes in the monoclinic crystal system, *P2/c* space group. Both imino groups are protonated. The proton migrates from the phenolic group to the imino group. Both manganese ions show a coordination number of 6, with an octahedral stereochemistry (Figure 7). The coordination sphere is made by 6 oxygen atoms arising from two chelating $hfac^-$ ligands, one aminoxyl oxygen, and one phenoxido oxygen, with distances varying between 2.114(2) and 2.176(3) Å. The intramolecular distance between the Mn(II) ions is 8.028 Å.

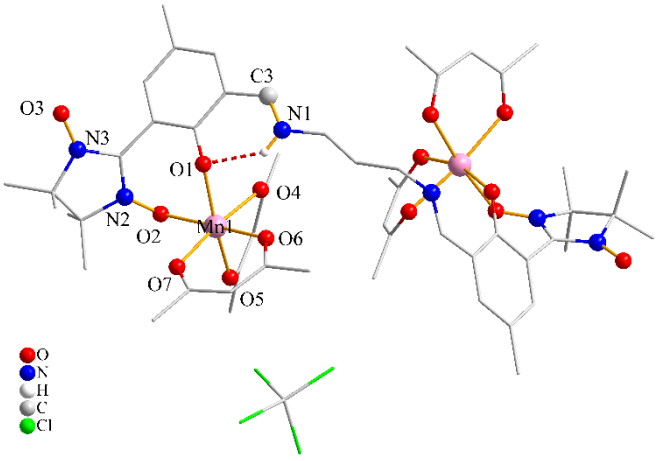

Figure 7. View of the molecular structure of $[Mn_2(L^9H_2)(hfac)_4]\cdot CH_2Cl_2$ (**54**). Florine atoms and a part of hydrogen atoms have been omitted for clarity. The dichloromethane molecule is disordered on two crystallographic positions. The two halves of the molecule are identical.

The magnetic behavior of compound **54** have been evaluated in the absence of the solvent molecule. At room temperature a $\chi_M T$ value of 6.62 cm^3 K mol^{-1} is observed, which is significantly lower than the expected value of 9.50 cm^3 K mol^{-1} for uncoupled spins with $S_1 = S_3 = {}^5/_2$ and $S_2 = S_4 = {}^1/_2$. By cooling down to 18 K, a moderate decrease to 6.03 cm^3 K mol^{-1} of the $\chi_M T$ product is observed. Further cooling leads to a sharp increase to 6.25 cm^3 K mol^{-1} (Figure 8). The magnetisation curves saturate at 7.59 $N\mu_B$ at low temperatures and high field, while no nesting of the iso-field magnetisation curves can be observed, indicating an isotropic system. The magnetic data can be simulated satisfactorily only taking into account an antiferromagnetic interaction between the radical and the manganese ion. Simultaneous simulation of the temperature dependent susceptibility and field dependent magnetisation data gives $J_{13} = J_{24} = -82.0(4)$ cm^{-1} and $g_{all} = 2.00$. A very small ferromagnetic mean filed

interaction of zJ = +0.0034(2) cm^{-1} has to be taken into account the obtain a good simulation of the very low temperature data.

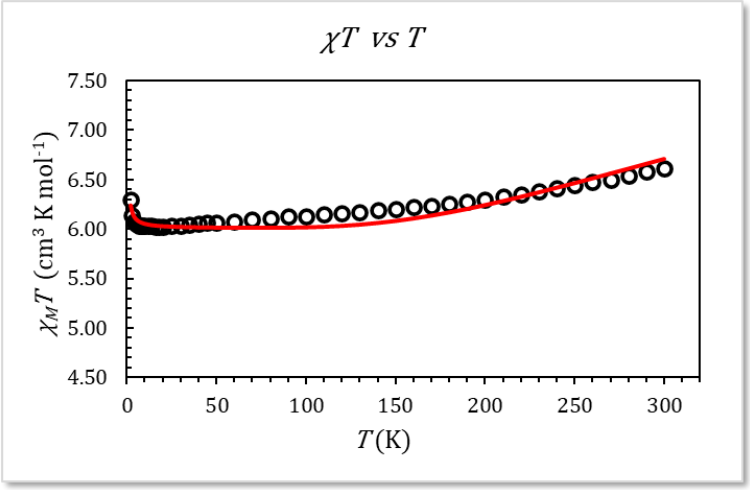

Figure 8. Temperature dependence of the molar susceptibility depicted in $\chi_M T$ *vs* T for **54**. The solid line corresponds to the best fit obtained with the parameter described in the text.

The magnetic properties were also investigated for the Gd(III) mononuclear complexes containing the ligands **H$_2$L^8** and **HL^{10}**. In both cases, crystallographic analysis reveals that only one of the two radical moieties present in each ligand coordinates to the metal center, in accordance with the synthetic design (Figure 9).

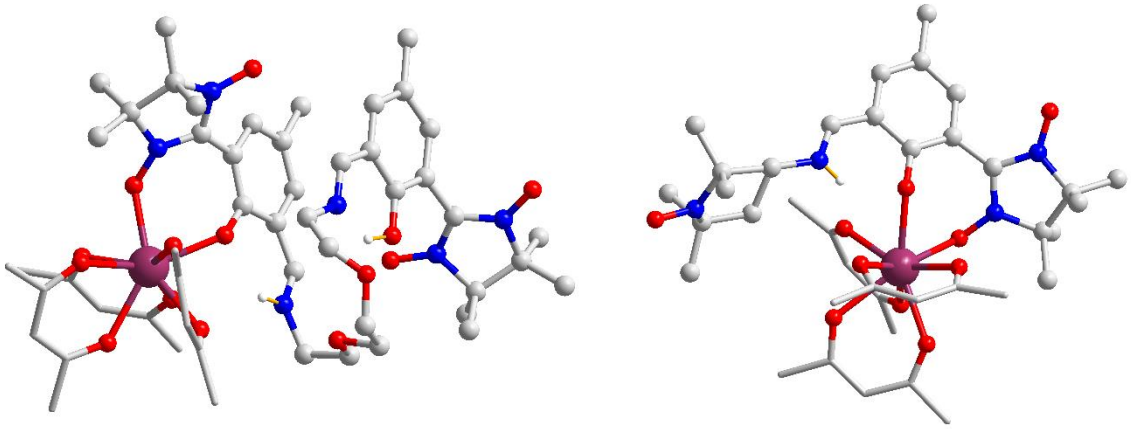

Figure 9. View of the crystal structures of [Gd(HL^{8}H)(hfac)$_3$], **48** (left) and of [Gd(L^{10}H)(hfac)$_3$], **61** (right). A part of the hydrogen atoms and all fluorine atoms were removed for clarity.

The temperature dependence of the $\chi_M T$ product has been recorded for compound **48** (Figure 10). Based on the crystal structure (Figure 9), one NN moiety is directly coordinated to the Gd(III) ion, while the second NN moiety remains non-coordinated, indicating the absence of significant intramolecular magnetic coupling. The magnetic susceptibility of compound **48** was measured over the temperature range 1.8–300 K. At room temperature, the $\chi_M T$ value is 8.49 cm^3 mol^{-1} K, in good agreement with the theoretical value of 8.625 cm^3 mol^{-1} K expected for a system comprising a Gd(III) ion (S = 7/2) and two S = 1/2 radical

centers in the absence of exchange interactions. Upon cooling, the $\chi_M T$ product increases, reaching a maximum of 9.99 cm³ mol⁻¹ K at 11 K, and subsequently decreases sharply to 9.02 cm³ mol⁻¹ K at 1.8 K (Figure 10).

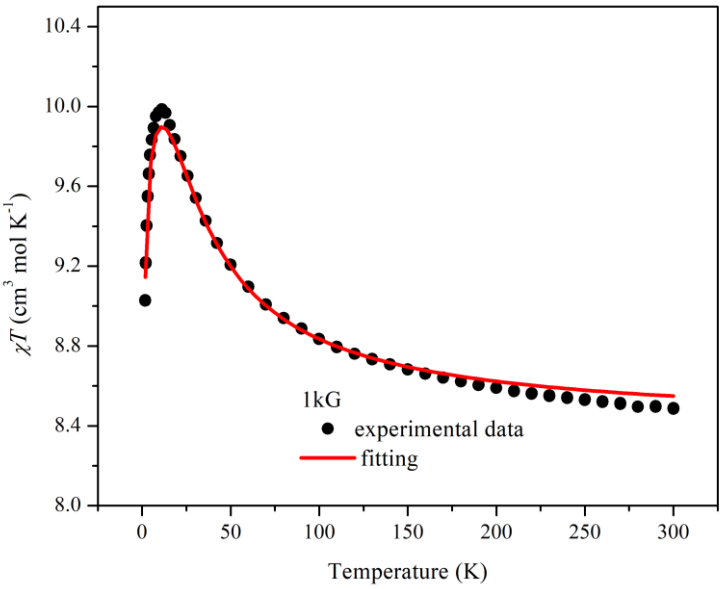

Figure 10. Temperature dependence the $\chi_M T$ product for compound **48**. With dots are represented the experimental values and with red line the best fitting.

The magnetic data were analyzed using the spin-only model described by Equation 1, based on the spin Hamiltonian $\hat{H} = -2J\mathbf{S}_{\mathrm{NN}} \cdot \mathbf{S}_{\mathrm{Gd}}$. Contributions from orbital angular momentum and magnetic anisotropy were neglected, consistent with the electronic configuration of the Gd(III) ion. In Equation 1, N denotes Avogadro's number, β the Bohr magneton, k the Boltzmann constant, T the temperature, g_1 the Landé g-factor of Gd(III), g_2 the Landé g-factor of the NN radical (fixed at 2.00), J the exchange coupling constant, and θ the Weiss constant.

$$\chi_M T = \frac{4Ng_1^2\beta^2}{k}\frac{T}{T-\theta}\left[\frac{15+7\,exp\left(-\frac{8J}{kT}\right)}{9+7exp\,(-\frac{8J}{kT})}\right] + \frac{Ng_2^2\beta^2}{4\kappa}\frac{T}{T-\theta} \qquad (1)$$

The least-squares fitting of the experimental magnetic susceptibility data yielded the following parameters: J = 4.34 cm^{-1}, g_1 = 1.97 and θ = -0.19 K. The positive J value indicates ferromagnetic coupling between the Gd(III) ion and the NN radical. In contrast, the negative Weiss constant suggests weak antiferromagnetic interactions between neighboring molecules of compound **48**. Consistent with this fact, the packing diagram reveals a close contact

between the uncoordinated NN moiety of one complex unit and the coordinated NN moiety of an adjacent molecule, with an O6···O3^{i} = 4.63 Å (Figure 11).

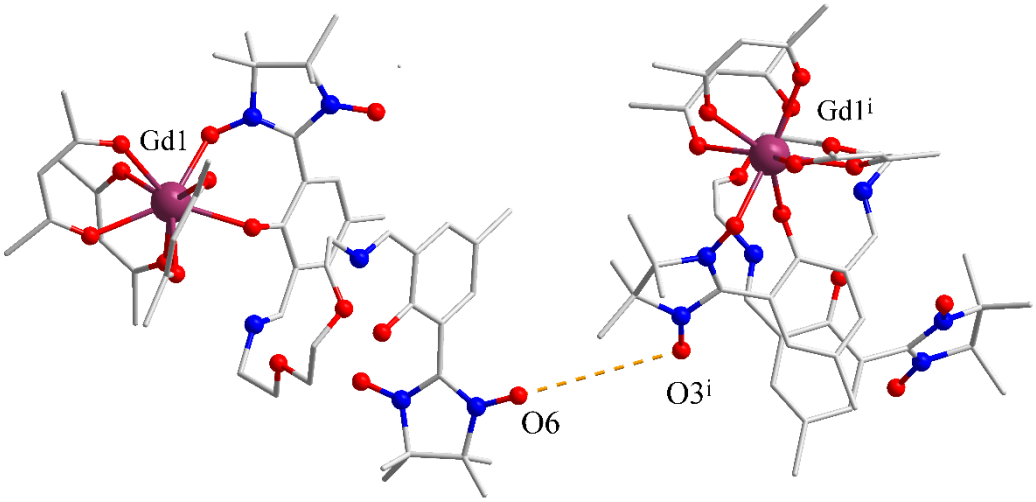

Figure 11. View of the two neighboring molecules of **48** with the radical moieties in close vicinity. The hydrogen and fluorine atoms have been omitted for clarity. Symmetry operation: i = 2-*x*, ½+*y*, *3/2-z*.

***

Extensive and redundant experimental data are organized into nine appendices, providing comprehensive details on synthetic procedures, crystallographic tables, and powder X-ray diffraction patterns. These sections include SHAPE analysis, magnetic characterization, and spectroscopic data (EPR, MS, and NMR), alongside DFT calculations.

This work explores the development of novel paramagnetic nitronyl nitroxide ligands featuring diverse coordination site topologies. It details the synthesis and characterization of mono- and dinuclear heterospin complexes incorporating d or f block metal ions with various spin architectures. To gain deeper insight into these chemical systems, several synthetic byproducts were rigorously analyzed. Additionally, the study describes the design of a new family of Schiff-base nitronyl nitroxide (Schiff-NN) ligands and their corresponding coordination complexes

The present work comprises more than 35 newly synthesized ligands and over 130 measured and solved crystal structures, and it opens new opportunity for rational design of nitronyl nitroxide ligands with specific biding sites and selected number of radical units. Part of the results of this research has been disseminated through five research articles:

- A New Nitronyl-Nitroxide Ligand for Designing Binuclear Ln^{III} Complexes: Syntheses, Crystal Structures, Magnetic and EPR Studies, **Mihai Răducă**, Daniel O. T. A. Martins, Cristian A. Spinu, Mihaela Hillebrand, Floriana Tuna, Gabriela Ionita, Augustin M. Mădălan, Constance

Lecourt, Jean-Pascal Sutter, Marius Andruh, *Eur. J. Inorg. Chem.*, **2022**, https://doi.org/10.1002/ejic.202200128

- SYNTHESES AND CRYSTAL STRUCTURES OF YTTRIUM AND DYSPROSIUM TETRAKIS(HEXAFLUOROACETYLACETONATO) WITH TRIETHYLAMMONIUM COUNTERION, **Mihai Răducă**, Marius-Mihai Zaharia and Marius Andruh, *Revue Roumaine de Chimie*, **2023**, DOI: 10.33224/rrch.2023.68.5-6.03
- ALKYLATION OF MORPHOLINE WITH 2-(CHLOROMETHYL)-NITROXYL-NITROXIDE: A NEW LIGAND AND ITS NICKEL COMPLEX, Ștefan Dimitriu, **Mihai Răducă**, Victoriția Tecuceanu, Anamaria Hanganu and Marius Andruh, *Revue Roumaine de Chimie*, **2024**, *69*, 279, DOI: 10.33224/rrch.2024.69.5-6.05
- A Cobalt(II)-nitronyl nitroxide single chain magnet with record blocking temperature and low coercivity, Thomaz de A. Costa, **Mihai Răducă**, Julio C. Rocha, Miguel A. Novak, Rafael A. A. Cassaro, Marius Andruh and Maria G. F. Vaz, *Inorganic Chemistry Frontiers*, **2025**, https://doi.org/10.1039/D4QI02703E
- Functionalization of nitronyl-nitroxide ligands via Schiff condensations. Rational synthesis of binuclear complexes with bis-nitronyl-nitroxide ligands, **Mihai Răducă**, Luca M. Carrella, Gabriela Ionita, Alexandru-Tudor Toderașc, Eva Rentschler, Marius Andruh, *Crystal Growth & Design*, **2025**, https://doi.org/10.1021/acs.cgd.5c01224

In the foreseeable future, I aim to continue the magnetic investigation of the compounds presented and to develop new complexes incorporating the paramagnetic organic molecules described herein that have not yet been employed as ligands. Furthermore, by applying the established synthetic techniques, I seek to modulate the distances between radical units within diradical molecules in order to obtain materials exhibiting qubit and quantum gate properties. Also, the ligands described will be used to construct heteronuclear complexes embodying both transitional and lanthanide ions. Future efforts will focus on the targeted synthesis of f-f' heterometallic complexes coordinated with paramagnetic ligands. Establishing a rational synthetic pathway for these species remains a key challenge, particularly regarding the controlled assembly of different lanthanide ions within a single molecular framework.